Bulletin of Entomological Research (2018) **108**, 807–816
doi:10.1017/S0007485318000068

Identification and tissue expression profiling of candidate UDP-glycosyltransferase genes expressed in *Holotrichia parallela* motschulsky antennae

S. Wang[1], Y. Liu[1], J.-J. Zhou[2], J.-K. Yi[1], Y. Pan[1], J. Wang[1], X.-X. Zhang[1], J.-X. Wang[1], S. Yang[1] and J.-H. Xi[1]*

[1]College of Plant Science, Jilin University, Changchun 130062, P.R. China:
[2]Department of Biointeractions and Crop Protection, Rothamsted Research, Harpenden AL5 2JQ, UK

Abstract

It is difficult to control *Holotrichia parallela* Motschulsky with chemical insecticides due to the larvae's soil-living habit, thus the pest has caused great economic losses in agriculture. In addition, uridine diphosphate-glycosyltransferases (UGTs) catalyze the glycosylation process of a variety of small lipophilic molecules with sugars to produce water-soluble glycosides, and play multiple roles in detoxification, endobiotic modulation, and sequestration in an insect. Some UGTs were found specifically expressed in antennae of *Drosophila melanogaster* and *Spodoptera littoralis*, and glucurono-conjugated odorants could not elicit any olfactory signals, suggesting that the UGTs may play roles in odorant inactivation by biotransformation. In the current study, we performed a genome-wide analysis of the candidate UGT family in the dark black chafer, *H. parallela*. Based on a UGT gene signature and the similarity of these genes to UGT homologs from other organisms, 20 putative *H. parallela* UGT genes were identified. Bioinformatics analysis was used to predict sequence and structural features of *H. parallela* UGT proteins, and revealed important domains and residues involved in sugar donor binding and catalysis by comparison with human UGT2B7. Phylogenetic analysis of these 20 UGT protein sequences revealed eight major groups, including both order-specific and conserved groups, which are common to more than one order. Of these 20 UGT genes, *HparUGT1265-1*, *HparUGT3119*, and *HparUGT*8312 were highly (>100-fold change) expressed in antennae, suggesting a possible role in olfactory tissue, and most likely in odorant inactivation and olfactory processing. The remaining UGT genes were expressed in all tissues (head, thorax, abdomen, leg, and wing), indicating that these UGTs likely have different biological functions. This study provides the fundamental basis for determining the function of UGTs in a highly specialized olfactory organ, the *H. parallela* antenna.

Keywords: UDP-glycosyltransferase, *Holotrichia parallela*, antennae, olfaction

(Accepted 30 December 2017; First published online 5 February 2018)

Introduction

In insects, odorant reception occurs mainly in the antennae via hair-like structures called olfactory sensilla. These morphofunctional units enclose olfactory receptor neurons, which are surrounded by a protein-enriched lymph. Detection of olfactory molecules (compounds) at the peripheral level is a complex

*Author for correspondence
Phone: +86-13756072796
Fax: +86-431-87836255
E-mail: jhxi1965@jlu.edu.cn

process involving numerous molecular actors (Durand *et al.*, 2010; Zhou, 2010; Zhou *et al.*, 2010). This includes the binding and transport of hydrophobic odorant molecules by odorant-binding proteins (OBPs), their recognition by odorant receptors (ORs) and their inactivation through hydrolysis by specific enzymes such as the odorant-degrading enzymes (ODEs) (Rützler & Zwiebel, 2005). The rapid inactivation of signals by ODEs plays an integral role in insect chemoreception, which prevents the accumulation of stimulants and subsequent sensory adaptation (Vogt & Riddiford, 1981), and allows insects to rapidly respond to changes in chemical volatiles in the environment. Several enzymes are known to be involved in such mechanisms, including cytochrome P450s, certain esterases, glutathione S-transferases (GSTs), members of the short-chain dehydrogenase/reductase family (aldehyde oxidases and alcohol dehydrogenases) and uridine diphosphate (UDP)-glycosyltransferases (UGTs) (Younus *et al.*, 2014). Compared to other ODE families, such as esterases, there are limited published reports on UGTs that are involved in insect olfaction.

Glycoside conjugation is an important metabolic pathway for the biotransformation of a variety of lipophilic xenobiotics and endobiotics (Bozzolan *et al.*, 2014). UGTs can convert lipophilic aglycones into more hydrophilic glycosides by catalyzing the conjugation of a glycosyl group donated by a UDP-glycoside to various small hydrophobic molecules. Through this process, UGTs facilitate the excretion of hydrophobic compounds and protect the cell from being damaged by toxic hydrophobic compounds to maintain proper intracellular regulation (Ahn *et al.*, 2011, 2012). In insects, the significance of the glycosylation of small hydrophobic compounds has been overlooked for many years, although recently, insect UGTs have been suggested to play multiple roles in the detoxification and sequestration of a variety of plant allelochemicals and insecticides (Kojima *et al.*, 2010; Ahn *et al.*, 2011). Of note, recent findings have revealed that insect UGTs are implicated in the termination of olfactory signals (Ahn *et al.*, 2012; Younus *et al.*, 2014).

The role of UGTs in vertebrate olfaction is well established (Heydel *et al.*, 2001). UGT2A1, which is highly expressed in the rat olfactory epithelium (Zhang *et al.*, 2005), can conjugate odorants, and terminate the odorant signals (Lazard *et al.*, 1991). However, in insects, evidence on UGT expression in the antennae is limited to three species, *Drosophila melanogaster* (Wang *et al.*, 1999), *Bombyx mori* (Huang *et al.*, 2008) and *Manduca sexta* (Robertson *et al.*, 1999), suggesting a possible role in olfactory processing. Two UGTs, UGT35a, and UGT35b, have previously been shown to be preferentially expressed in the third antennal segment of *D. melanogaster*, and the latter was suggested to be possibly involved in odorant turnover (Wang *et al.*, 1999). Because of the rich diversity and the variety of the possible functions of detoxification enzymes expressed in each species, the identification and characterization of individual members of these enzyme families, which are each specialized in odorant degradation within the antennae, are still challenging (Younus *et al.*, 2014).

The dark black chafer, *Holotrichia parallela* Motschulsky (Coleoptera: Scarabaeidae), is one of the most important soil pests worldwide (Ju *et al.*, 2014). In China, *H. parallela* has caused a significant loss in crop yields and great economic damage by attacking crops, vegetables and economically important trees (Ju *et al.*, 2014; Zhang *et al.*, 2016). Because *H. parallela* larvae live in the soil, it is difficult to control them using traditional pesticides. Chemical communication is so crucial for the interaction of *H. parallela* with their environment that olfactory-related gene products could be effectively utilized as new targets to reduce insect populations (Ju *et al.*, 2012).

In this study, 20 putative UGT genes were identified from the *H. parallela* antennae transcriptome. We describe the sequence and phylogenetic analyses of *H. parallela* antennae UGTs and predict the corresponding UGT protein structures. This study also elucidates UGT expression patterns in different tissues. These findings serve as an important basis for the identification of *H. parallela* UGTs that participate in odorant degradation.

Method

Insect and tissue collection

H. parallela strains used in this study were collected in Cangzhou, China. The antennae, heads, thoraces, abdomens, legs, and wings of male and female adults were dissected and promptly immersed in liquid nitrogen and stored at −80°C until use (Wang *et al.*, 2017).

Identification of UDP-glycosyltransferases genes from H. parallela

H. parallela antennae transcriptome data used in this study are from our laboratory (data not shown). UDP-glycosyltransferase genes were selected by searching the sequences in the antennal transcriptome database and annotations for keywords (UDP-glycosyltransferases). Subsequently, UGT conserved domains (UDPGT) of the selected *H. parallela* UGT genes were further predicted using the Pfam database (http://pfam.xfam.org). For possible alternatively spliced genes, only the longest coding transcript was selected.

Bioinformatic analyses

Open reading frames (ORFs) of genes were predicted using ORF finder (http://www.ncbi.nlm.nih.gov/gorf/gorf.html). Theoretical isoelectric points and molecular weights of deduced proteins were calculated using the ExPASy Compute pI/Mw tool (http://web.expasy.org/compute_pi/) (Gasteiger *et al.*, 2003). Signal peptides and transmembrane domains were predicted using SignalP 4.1 (http://www.cbs.dtu.dk/services/SignalP/) (Petersen *et al.*, 2011) and TMHMM2.0 (http://www.cbs.dtu.dk/services/TMHMM), respectively. Amino acid sequence multiple alignments were analyzed by using DNAMAN software (http://www.lynnon.com/pc/alignm.html) with default parameters (Duan *et al.*, 2016). SWISS-MODEL (http://swissmodel.expasy.org/), which is available within ExPASy, were used to predict tertiary structures (Biasini *et al.*, 2014). BLASTX best hits were found using the BLASTX program, provided by NCBI (http://blast.ncbi.nlm.nih.gov/Blast.cgi) (Altschul *et al.*, 1997). The neighbor-joining phylogenetic tree was constructed by MEGA6 using the p-distance metric at bootstrap 1000 (Ahn *et al.*, 2012; Tamura *et al.*, 2013).

RNA isolation and cDNA synthesis

Total RNA was extracted from different tissues (antennae, heads, thoraces, abdomens, legs, and wings) using RNAiso Plus (Takara, Dalian, China) following the manufacturer's protocol. Total RNA was quantified and checked for purity and integrity using a NanoDrop 2000 Spectrophotometer

https://doi.org/10.1017/S0007485318000068 Published online by Cambridge University Press

(Thermo Fisher Scientific, Wilmington, DE) and gel electrophoresis. PrimeScript™ RT reagent Kit with gDNA Eraser (RR047A, Takara, Dalian, China) was used for cDNA synthesis.

Quantitative real-time polymerase chain reaction (qPCR)

Primer pairs for qPCR were designed using Primer 5 software and are listed in Supplementary table 2. GAPDH was used as a reference gene (Zhang *et al*., 2016). mRNA levels were measured by qPCR using the SYBR® Premix Ex Taq™ (Takara, Dalian, China). Each amplification reaction contained 1 µl of cDNA, 10 µl of SYBR Premix Ex Taq, 0.4 µl of 10 µM of forward primer, 0.4 µl of reverse primer, 0.4 µl of ROX Reference Dye II and 7.8 µl water in a 20 µl total volume. qPCR was performed on an ABI 7500 Real-Time PCR System (Applied Biosystems, Carlsbad, CA, USA) under the following conditions: 30 s initial denaturation at 95°C and 40 cycles of 95°C for 5 s, 60°C for 10 s and 72°C for 34 s, followed by the melting curve analysis (60–95°C). After qPCR, melting curves were evaluated to confirm single peaks and check amplification specificity. Means and standard errors were obtained from the average of three biological replicates with their three respective technical replicates. The fold changes were evaluated using the $2^{-\Delta\Delta Ct}$ method (Pfaffl, 2001). Statistical analysis was conducted using GraphPad Prism 5 software (San Diego, CA).

Results

Identification of 20 putative UGTs

To identify olfaction-related genes and explore the olfactory signal transduction mechanisms in *H. parallela*, the *H. parallela* antennal transcriptome sequencing from adult females and males was conducted. Female antennae transcripts were assembled into 71,928 Contigs and 43,624 unigenes, and male antennae transcripts were assembled into 63,485 Contigs and 38,785 unigenes. A total of 19025 unigenes (54.82% of all unigenes) returned the annotation result by searching against non-redundant (NR), Swissprot, KEGG, COG, and GO databases with a cut-off E-value of 10^{-5}. Of them, 47 candidate OR genes and 26 OBP genes were identified in the male and female antennal transcriptomes (unpublished). In this paper, a total of 20 cDNA fragments encoding putative UGTs were identified from the *H. parallela* antennal transcriptome, with gene lengths between 1009 and 2777 bp (table 1). These 20 cDNAs all have predicted UDPGT domains with low *E*-values (6.2×10^{-66}–$3.3-10^{-90}$) based on Pfam. Of these, 15 sequences have complete ORFs, while four sequences (*HparUGT1625-1*, *HparUGT1630*, *HparUGT5694*, *and HparUGT7488*) are incomplete sequences truncated at 5′-regions, and one sequence (*HparUGT15028*) contains a truncated 3′-region. The lengths of the 15 deduced full-length UGT proteins range from 505 to 524 amino acids, with predicted isoelectric points ranging from pI 5.83 to 9.28 and calculated molecular masses between 57.99 and 59.71 KDa.

Structural prediction of UGT proteins

Sequence alignments combined with multiple bioinformatics methods revealed the major structural features of the putative *H. parallela* UGT proteins (fig. 1). In general, the N-terminal half is highly variable, whereas the C-terminal half is more conserved. All identified *H. parallela* UGT proteins, including the truncated UGT proteins, displayed the characteristic UGT signature motif in the middle of the C-terminal domain. Signal peptides were detected in 14 *H. parallela* UGT proteins but not in the four sequences with incomplete N-terminal regions (fig. 1). In addition, transmembrane domains, followed by cytoplasmic tails, were also identified at the C-terminal of all *H. parallela* UGTs. A highly conserved aspartate residue, which is a negatively charged amino acid residue, is immediately in front of the transmembrane domain on the luminal side. Based on comparison with the crystal structure of human UGT2B7, there are two predicted sugar binding regions (DBR1 and DBR2) observed in the *H. parallela* UGT proteins, and several important residues that interact with

Table 1. Summary of *H. parallela* antennal UGTs sequences.

Gene ID	Gene Length	ORF(aa)	Mw (kDa)	PI	SP	Domains	Pfam *E*-value	N-glycosylation predicted sites
HparUGT10995	1748	513	58.64	8.99	Yes	UDPGT	4.80×10^{-70}	4,17,51,66,167,245
HparUGT1265-1	1353	>404	46.56	8.18	No	UDPGT	2.30×10^{-73}	19,64,129
HparUGT1265-3	1725	507	58.76	7.78	Yes	UDPGT	5.00×10^{-73}	122,167,232,405,459
HparUGT12965	1853	510	59.31	8.08	Yes	UDPGT	3.40×10^{-70}	48,63,312
HparUGT15028	1560	>504	57.73	8.10	Yes	UDPGT	1.80×10^{-79}	233,268,460
HparUGT1601-3	1817	508	59.12	8.40	Yes	UDPGT	1.90×10^{-70}	48,63,310
HparUGT1601-4	1613	510	59.39	5.83	Yes	UDPGT	2.50×10^{-67}	48,63,183,277,312
HparUGT1601-6	2777	511	59.44	6.79	Yes	UDPGT	8.40×10^{-73}	48,63,180,222,313,453
HparUGT1605	1775	512	58.92	5.83	No	UDPGT	1.30×10^{-79}	48,63,181,454,464
HparUGT1630	1009	>323	37.01	9.12	No	UDPGT	2.60×10^{-68}	48
HparUGT1646	1675	508	58.51	9.28	Yes	UDPGT	5.90×10^{-70}	123,233,406,460
HparUGT3119	1800	513	59.08	8.64	Yes	UDPGT	6.20×10^{-66}	4964
HparUGT366	1711	524	59.71	8.40	Yes	UDPGT	9.40×10^{-87}	52,82,173,239
HparUGT3727	1545	507	58.06	9.20	Yes	UDPGT	2.50×10^{-66}	63,167,184,233,297,400
HparUGT5658	1559	507	58.28	6.71	Yes	UDPGT	1.20×10^{-74}	47,62,653
HparUGT5694	1796	>279	31.88	8.83	No	UDPGT	4.10×10^{-75}	39,169
HparUGT7488	1679	>460	52.65	8.94	No	UDPGT	1.20×10^{-84}	184
HparUGT8131	2221	518	59.01	7.25	No	UDPGT	5.50×10^{-71}	51,66,246,295
HparUGT8312	2078	509	59.24	8.36	Yes	UDPGT	9.40×10^{-76}	124,169,234
HparUGT9114	1842	505	57.99	9.13	Yes	UDPGT	3.30×10^{-90}	166,227,273,318

ORF, open reading frame; MW, molecular weight; PI, isoelectric point; SP, signal peptide.

https://doi.org/10.1017/S0007485318000068 Published online by Cambridge University Press

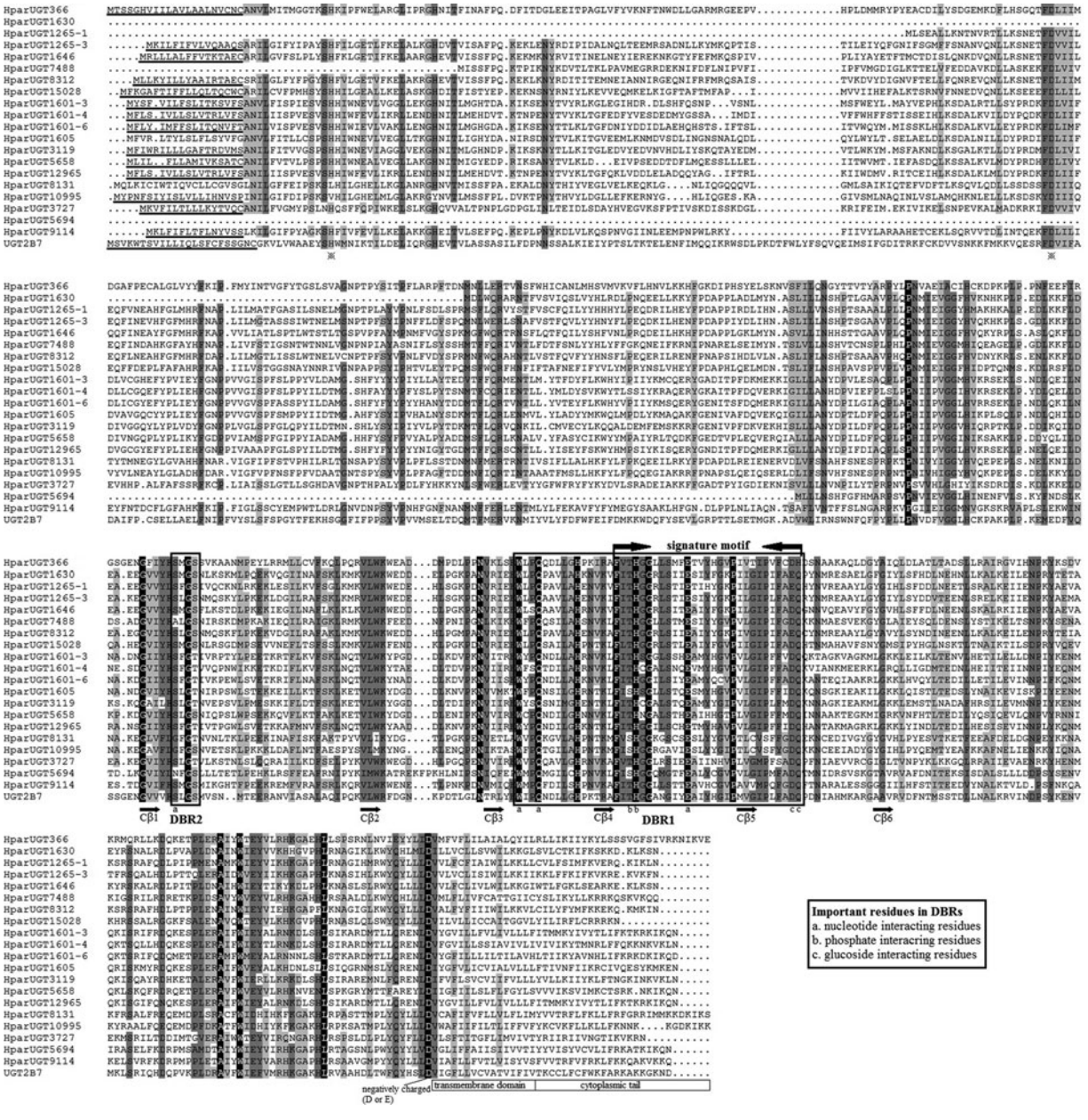

Fig. 1. Multiple alignment of 20 *H. parallela* UGTs with human UGT2B7. The N-terminal signal peptides predicted by SignalP 4.1 are underlined. The transmembrane domain and cytoplasmic tails based on human UGT2B7 (accession number NM_001074) are in white boxes under alignment. The signature motif is indicated by arrows above the alignment. All of the putative β-sheets in the C-terminal half predicted by comparison with human UGT2B7 crystal structure are denoted as Cβ + number with an arrow. Asterisks (※) below the alignment indicate the important catalytic residues (H and D). Two donor binding regions (DBR) are boxed and several important residues interacting with the sugar donor are indicated by letters (a,b and c) below the alignment.

the sugar donor are also conserved (fig. 1). Finally, the two catalytic residues located in the N-terminal substrate binding site are also evolutionarily conserved between two species (fig. 1). In addition, the three-dimensional structure of *HparUGT1646*, the highest homologous UGT of *H. parallela* with human UGT2B7, was predicted using human UGT2B7 as a template (fig. 2), confirming these homologous features between two proteins.

Homology and phylogenetic analysis

The 20 *H. parallela* UGTs as well as the UGTs from *Tribolium castaneum*, *B. mori*, *Aedes aegypti*, and *Apis mellifera* distribute into 8 major groups (group A-H) that localize to distinct branches of the phylogenetic tree (fig. 3). The phylogenetic tree contains some order-specific groups, such as the Lepidoptera- (D), Coleoptera- (A), and Diptera-specific groups

https://doi.org/10.1017/S0007485318000068 Published online by Cambridge University Press

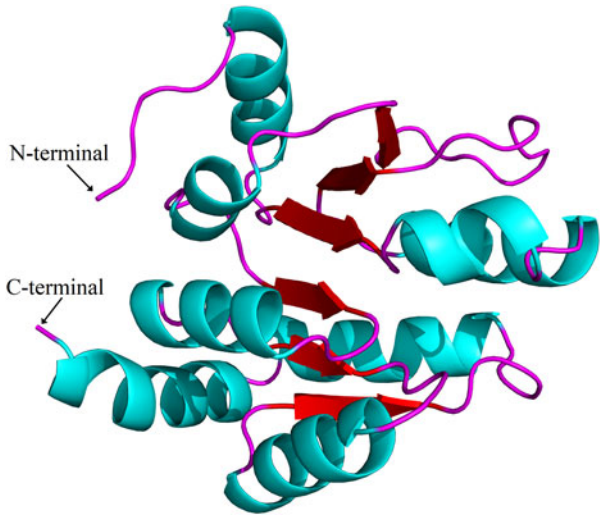

Fig. 2. Putative three-dimensional structure of HparUGT1646, the highest homologous UGT of *H. parallela* with human UGT2B7. The three-dimensional structure was predicted using human UGT2B7 as the template.

(B), and several conserved groups which are common to more than one order (C, E, F, G, and H). Most groups are supported by high bootstrap values. The *H. parallela* UGTs belong to five groups and fall into a branch together with the *T. castaneum* UGTs. The largest group, Group A, contains nine *H. parallela* UGT genes. Group F is the second largest group and contains seven members. The remaining groups, E and F, contain two members and a single member, respectively. The phylogenetic tree is reconstructed by Maximum likelihood methods (Supplementary fig. 1). The cluster pattern of a phylogenetic tree, reconstructed by Maximum likelihood methods, is quite similar to that of the neighbor-joining phylogenetic tree, verifying the reliability of neighbor-joining phylogenetic tree. Consistent with this phylogenetic tree, BLASTX best hits analysis of the *H. parallela* UGTs showed that their respective orthologs are all sequences from *T. castaneum* with sequence identities ranging from 37 to 70% and *E*-values from 0 to 4×10^{-95} (table 2). Of the 15 full-length UGTs, *HparUGT366* shared the highest identity (70%) with the *T. castaneum* UGTs; 12 other *H. parallela* UGTs have identities ranging from 42 to 56%, and two remaining *H. parallela* UGTs have less than 40% identity with their respective orthologs.

Expression analysis of H. parallela *UGT genes*

Expression levels of *H. parallela* UGTs were determined in terms of fragments per kilobase of transcript per million mapped reads (FPKM) estimated from the antennae RNA-seq data (table 3). Except *HparUGT366*, all UGTs were found to be expressed in antennae at FPKM>1, and 11 of them had an FPKM>10 in male or female antennae. Compared to other UGTs, *HparUGT3119* showed the highest expression in both female and male antennae, with FPKM = 1024.8755 and FPKM = 972.9668, respectively (table 3). *HparUGT9114* and *HparUGT7488* had an FPKM of >100 in at least one of the female or male antennae.

qPCR analysis revealed a wide range of expression patterns of the *H. parallela* UGTs in different tissues (fig. 4), including antennae and various non-olfactory tissues. Most *H. parallela* UGTs were ubiquitously expressed in most tissues, although some *H. parallela* UGTs were preferentially expressed in a specific tissue. Of note, *HparUGT1265-1*, *HparUGT3119*, and *HparUGT8312* were restricted to the antennae and barely detectable in other tissues. In addition to antennae, *HparUGT366*, *HparUGT1265-3*, *HparUGT7488*, *HparUGT1601-6*, *HparUGT 12965*, *HparUGT10995*, *HparUGT8131*, *HparUGT9114*, and *HparUGT3727* were highly expressed in other tissues. Of the remaining UGTs, *HparUGT1601-3* was mainly expressed in the thorax, *HparUGT1646* was mainly expressed in the wings and *HparUGT5694* in the heads. *HparUGT1630* and *HparUGT1601-4* were highly expressed in both the abdomen and thorax.

Discussion

Based on the previous genome-wide analysis, UGT gene numbers ranging from 12 to 58 have been identified in various insect species including *B. mori* (45), *T. castaneum* (43), three *Diptera* species, two *Hymenoptera* species and *Acyrthosiphon pisum* (58). In addition, 45 *H. armigera* UGTs were identified from RT-PCR analysis of a cDNA library (Ahn *et al.*, 2012). However, knowledge of UGT tissue distribution is limited. In this study, a total of 20 UGT members were identified from the *H. parallela* antennal transcriptome. This number of antennal UGTs in *H. parallela* is greater than that in *S. littoralis* (11 genes, Bozzolan *et al.*, 2014), suggesting that a large proportion of the *H. parallela* UGT repertoire has been detected by our transcriptome method. However, *T. castaneum* is known to have 43 UGTs, so other *H. parallela* UGTs might remain to be found. The high diversity of UGTs identified in *H. parallela* antennae likely reflects the functional importance of UGTs in antennae olfaction.

UDPGT domains were predicted with low E-values by Pfam software, and the UGT signature motif, a hallmark of prokaryotic and eukaryotic UGTs (Mackenzie *et al.*, 1997), was found in the *H. parallela* UGTs, strongly supporting these sequences as genes belonging to the UGT superfamily. As described for other insect UGTs (Ahn *et al.*, 2012), the *H. parallela* N-terminal substrate binding domain is less conserved than the C-terminal sugar donor binding domain. In a previous study, critical information regarding donor binding regions, sugar binding residues, and catalytic residues in insect UGTs was determined based on the crystal structures of human UGT2B7 and two plant UGTs (Miley *et al.*, 2007; Radominska-Pandya *et al.*, 2010; Ahn *et al.*, 2012). These key residues and donor binding regions are also conserved in *H. parallela* UGTs. In animals, a signal peptide found at the N-terminus of the UGT mediates the integration of the protein precursor into the endoplasmic reticulum (ER), and is subsequently cleaved. Then, the UGT is N-glycosylated and retained in the ER membrane by virtue of its hydrophobic transmembrane domain (Magdalou *et al.*, 2010). Similarly, we predicted N-glycosylation sites, signal peptides, and transmembrane domains for all of the *H. parallela* UGT sequences, and these features have also been reported in other insect UGTs (Bozzolan *et al.*, 2014). In summary, the structural features of *H. parallela* UGTs revealed by these data indicated that *H. parallela* UGTs were probably active enzymes with similar structures and functions to other known insect and animal UGTs.

The phylogenetic tree constructed in this study follows the phylogenetic pattern described previously for the insect UGTs (Ahn *et al.*, 2012). For example, the UGT50 family comprises

https://doi.org/10.1017/S0007485318000068 Published online by Cambridge University Press

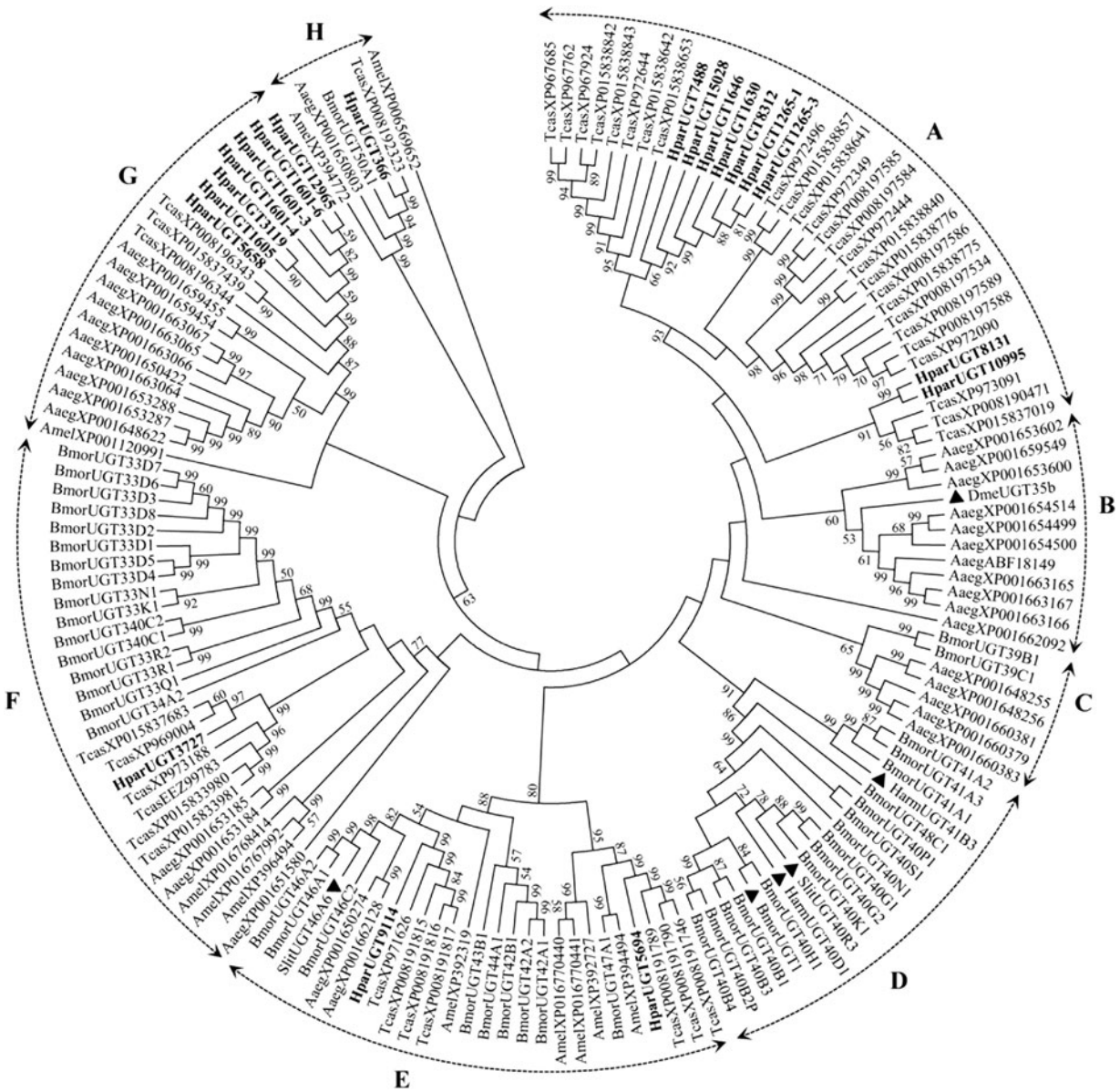

Fig. 3. Phylogenetic tree of *H. parallela* antennal UGTs with UGTs of other insects. Phylogenetic tree of UGT protein sequences from various insect species, including *H. parallela*, *T. castaneum*, *B. mori*, *A. aegypti*, *A. mellifera*, *Helicoverpa armigera*, *S. littoralis*, *D. melanogaster*. The GenBank accession numbers are included in the Supplemental table 2. Phylogenetic tree was constructed by MEGA 6 program using the neighbor-joining method with p-distance model and 1000 bootstrap replicates (Ahn *et al.*, 2012). Hpar, *H. parallela*; Tcas, *T. castaneum*; Bmor, *B. mori*; Aaeg, *A. aegypti*; Amel, *A. mellifera*; Harm, *H. armigera*; Slit, *S. littoralis*; Dme, *D. melanogaster*. The *H. parallela* UGTs are bold and the insect UGTs biochemically characterized were marked with black triangle. A-H represent eight major groups that localize to distinct branches of the phylogenetic tree, the phylogenetic pattern follows that described previously for the insect UGTs in the literature (Ahn *et al.*, 2012).

one member from each insect species, and includes *BmorUGT50A1* and *HparUGT366*. The genes within each group likely arose from a common ancestor and have a similar function. Phylogenetic analysis of plant UGTs has shown that phylogenetic grouping can be useful for predicting the substrates of a specific enzyme (Lim *et al.*, 2003; Cartwright *et al.*, 2008; Osmani *et al.*, 2009; Barvkar *et al.*, 2012). The predicted positions of the insect UGTs that have been characterized to some extent biochemically and were also superimposed onto the tree. Whereas *HarmUGT41B3* and *HarmUGT40D1* are capable of glycosylating gossypol (Krempl *et al.*, 2016), *BmorUGT1* catalyzes the glucosidation of a wide variety of substrates (Luque *et al.*, 2002), and *DmeUGT35b* and *SlitUGT4040R3* were preferentially expressed in olfactory organs of *D. melanogaster* and *S. littoralis* (Wang *et al.*, 1999; Bozzolan *et al.*, 2014). However, these UGTs do not provide clues to the function of *H. parallela* UGTs, as they belong to order-specific groups. Despite high

https://doi.org/10.1017/S0007485318000068 Published online by Cambridge University Press

Table 2. The BLASTX best hits summary of *H. parallela* antennal UGT genes.

Gene ID	Gene Name and Species	Query cover (%)	Value	Identities (%)	Accession
HparUGT10995	PREDICTED: UDP-glucuronosyltransferase 2C1-like (*Tribolium castaneum*)	80	3.00×10^{-107}	38	XP_008190471.1
HparUGT1265-1	PREDICTED: UDP-glucuronosyltransferase 2B16 (*Tribolium castaneum*)	94	5.00×10^{-133}	45	XP_967762.1
HparUGT1265-3	PREDICTED: UDP-glucuronosyltransferase (*Tribolium castaneum*)	81	1.00×10^{-146}	46	XP_967685.3
HparUGT12965	PREDICTED: UDP-glucuronosyltransferase 1-9 isoform X1 (*Tribolium castaneum*)	75	6.00×10^{-125}	45	XP_015837439.1
HparUGT15028	PREDICTED: UDP-glucuronosyltransferase (*Tribolium castaneum*)	84	1.00×10^{-133}	43	XP_967685.3
HparUGT1601-3	PREDICTED: UDP-glucuronosyltransferase 1-9 isoform X1 (*Tribolium castaneum*)	77	1.00×10^{-125}	44	XP_015837439.1
HparUGT1601-4	PREDICTED: UDP-glucuronosyltransferase 1-9 isoform X1 (*Tribolium castaneum*)	87	1.00×10^{-125}	43	XP_015837439.1
HparUGT1601-6	PREDICTED: UDP-glucuronosyltransferase 1-9 isoform X1 (*Tribolium castaneum*)	51	1.00×10^{-117}	44	XP_015837439.1
HparUGT1605	PREDICTED: UDP-glucuronosyltransferase 2B17 (*Tribolium castaneum*)	84	4.00×10^{-138}	42	XP_008196343.1
HparUGT1630	PREDICTED: UDP-glucuronosyltransferase (*Tribolium castaneum*)	92	1.00×10^{-109}	50	XP_967685.3
HparUGT1646	PREDICTED: UDP-glucuronosyltransferase 2B10-like (*Tribolium castaneum*)	82	1.00×10^{-120}	46	XP_972090.2
HparUGT3119	PREDICTED: UDP-glucuronosyltransferase 2B17 (*Tribolium castaneum*)	79	3.00×10^{-130}	42	XP_008196343.1
HparUGT366	PREDICTED: UDP-glucuronosyltransferase 2C1 (*Tribolium castaneum*)	90	0	70	XP_008192323.1
HparUGT3727	PREDICTED: UDP-glucuronosyltransferase 2B9 9 (*Tribolium castaneum*)	88	3.00×10^{-162}	50	XP_969004.1
HparUGT5658	PREDICTED: UDP-glucuronosyltransferase 2B17 (*Tribolium castaneum*)	97	3.00×10^{-138}	43	XP_008196343.1
HparUGT5694	UDP-glucuronosyltransferase 2B14-like Protein (*Tribolium castaneum*)	46	4.00×10^{-100}	60	EFA02010.1
HparUGT7488	PREDICTED: UDP-glucuronosyltransferase 2B16 (*Tribolium castaneum*)	81	2.00×10^{-159}	50	XP_967762.1
HparUGT8131	PREDICTED: UDP-glucuronosyltransferase-like (*Tribolium castaneum*)	63	4.00×10^{-95}	37	XP_015838642.1
HparUGT8312	PREDICTED: UDP-glucuronosyltransferase 2B10-like (*Tribolium castaneum*)	69	1.00×10^{-144}	46	XP_972090.2
HparUGT9114	PREDICTED: UDP-glucuronosyltransferase 1-7C isoform X4 (*Tribolium castaneum*)	80	0	56	XP_008191816.1

Table 3. Fragments per Kilobase per Million Mapped reads (FPKM) of *H. parallela* antennal UGTs estimated from antennae RNA-seq data.

Gene ID	Female antenna FPKM	Male antenna FPKM
HparUGT10995	54.8548	49.451
HparUGT1265-1	7.8039	15.3641
HparUGT1265-3	51.3294	41.1229
HparUGT12965	20.8837	16.6526
HparUGT15028	10.2042	7.4456
HparUGT1601-3	10.0293	9.3555
HparUGT1601-4	5.1504	4.5122
HparUGT1601-6	7.5465	5.8341
HparUGT1605	15.1583	14.8849
HparUGT1630	2.8153	2.4703
HparUGT1646	18.9112	18.9878
HparUGT3119	1024.8755	972.9668
HparUGT366	0.0627	0.4079
HparUGT3727	9.6788	8.389
HparUGT5658	8.3198	7.1306
HparUGT5694	3.0738	2.7756
HparUGT7488	103.4922	96.3752
HparUGT8131	20.3193	18.4722
HparUGT8312	1.5992	1.7752
HparUGT9114	274.9423	318.9119

homology with *T. castaneum* UGTs, *H. parallela* UGT functions cannot be determined by homology analysis due to limited reports on *T. castaneum* UGT catalytic activity. However, most *H. parallela* and *T. castaneum* UGTs share a common family or subfamily according to the current UGT nomenclature guidelines, which defines families and subfamilies as sharing at least 40 and 60% amino acid sequence identity (aaID), respectively (Mackenzie *et al.*, 2005).

The expression patterns of *H. parallela* UGTs may be useful to predict their functions. In vertebrates, *UGT2A1* is highly expressed in the rat olfactory epithelium, can glucuronidate odorants, and glucuronidation products abolish the ability of odorants to induce an olfactory response, suggesting that this olfactory-specific UGT participates in terminating odorant signals (Lazard *et al.*, 1991; Heydel *et al.*, 2001; Bozzolan *et al.*, 2014). The olfactory-restricted expression has been established as a useful criterion for identifying specific olfactory genes (Durand *et al.*, 2010; Bozzolan *et al.*, 2014) such as odorant-binding proteins, olfactory receptors, and some odorant-degrading enzymes (Benton *et al.*, 2007; Durand *et al.*, 2010). In this study, three genes (*HparUGT8312*, *HparUGT1265-1*, and *HparUGT3119*) were identified as being mainly expressed in antennae and are therefore implicated in a specific olfactory function. Indeed, several UGT genes that may be involved in specific roles in olfactory organs have also been found in other insects. For example, DmeUgt35b is preferentially expressed in the third antennal segment of *D. melanogaster*, and *UGT40R3* and *UGT46A6* are specifically expressed or overexpressed in antennae (Wang *et al.*, 1999; Bozzolan *et al.*, 2014). An increasing body of literature reported a possible involvement of UGTs in insect olfaction (Ahn *et al.*, 2012; Bozzolan *et al.*, 2014; Younus *et al.*, 2014). For example, preferential expression of UGT genes were also found in the antennae of *B. mori* (Huang *et al.*, 2008) and *M. sexta* (Robertson *et al.*, 1999). The powerful functions of UGTs in the metabolism of endogenous and exogenous compounds, resulting in the elimination and inactivation of their substrates, have also been shown in various insects (Luque *et al.*, 2002; Sasai *et al.*, 2009;

https://doi.org/10.1017/S0007485318000068 Published online by Cambridge University Press

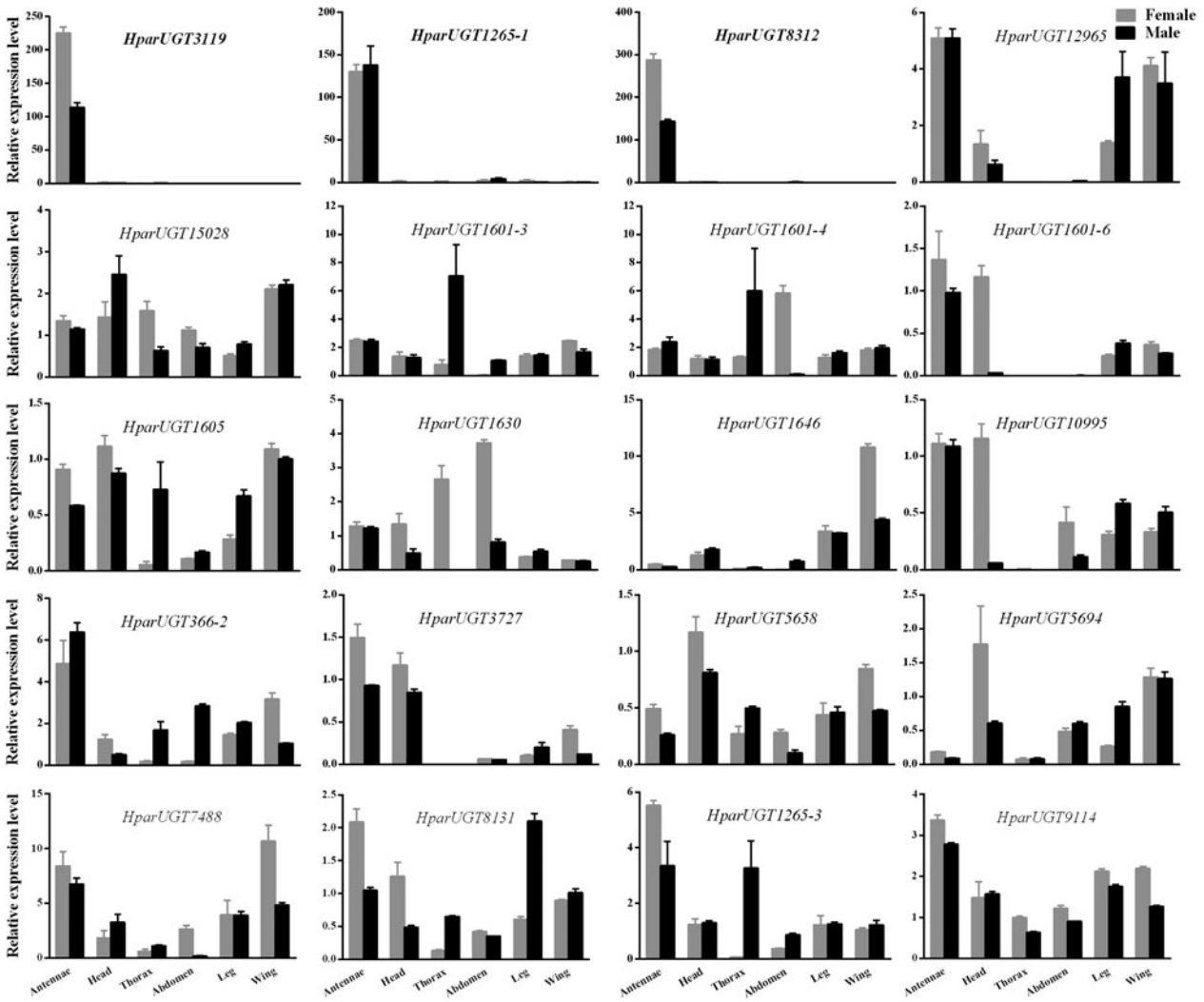

Fig. 4. Expression pattern of *H. parallela* antennal UGT genes by qPCR across various tissues. Fold changes were calculated using the $2^{-\Delta\Delta Ct}$ method. The gene expression levels in various tissues were normalized relative to that in female head. GADPH gene was used as the reference gene to normalize target gene expression. Data are shown as averages of biological and technical replicates ± SE of the mean. The three UGT genes (*HparUGT 3119*, *HparUGT1265-1* and *HparUGT 8312*), highlighted in bold in this figure, were highly expressed in antennae.

Ahn *et al.*, 2012; Bock, 2016) . Furthermore, it is worthy of note that the substrates of a UGT from *B. mori*, named BmUGT1, include a number of odorants, such as vanillin, eugenol, β-citronellol, isomenthol, *P*-hydroxybiphenyl, and guaiacol (Luque *et al.*, 2002). All these findings suggest that insect UGTs play possible roles in deactivation of olfactory signal, as already shown in vertebrate (Lazard *et al.*, 1991; Ahn *et al.*, 2012; Bozzolan *et al.*, 2014; Younus *et al.*, 2014). Interestingly, *SlitUGT46A6*, *HparUGT9114*, and *HparUGT5694* cluster in a conserved group (E) with a high bootstrap (80%). The antennal-specific *SliUGT46A6* exhibited upregulation or downregulation after insecticide or odorant exposure, respectively, suggesting its specific function in olfaction (Bozzolan *et al.*, 2014). The expression of UGTs in olfactory tissues was also reported in vertebrate (Heydel *et al.*, 2010; Olender *et al.*, 2016; Hanser *et al.*, 2017). For example, *UGT1A6* expressed in rat bulb, *UGT2A1* in the epithelium of bovine, mouse, and human (Heydel *et al.*, 2010). Furthermore, *UGT2A1* and *UGT2A2* have been detected in the rat olfactory sensory cilia, the important tissue in olfactory process (Lazard *et al.*, 1991; Mayer *et al.*, 2008; Heydel *et al.*, 2010, 2013).

Although we detected some *H. parallela* UGT genes in various non-olfactory tissues, suggesting that these genes may have other functions, they might still have olfactory functions, similar to how *SexiCXE13* and *SlituCXE13*, which are not antennae-specific genes, can also degrade sex pheromones and plant volatiles (He *et al.*, 2014). A UGT from *B. mori* exhibited a wide substrate specificity towards plant allelochemicals (Luque *et al.*, 2002). It is also reported that the glucuronidated small hydrophilic molecules disabled the ability of odorants to elicit an olfactory response (Lazard *et al.*, 1991; Leclerc *et al.*, 2002; Bozzolan *et al.*, 2014). Thus, the precise roles of *H. parallela* antennal UGTs in olfactory function awaits further investigation.

https://doi.org/10.1017/S0007485318000068 Published online by Cambridge University Press

Conclusions

In summary, a total of 20 UGT genes were identified from the *H. parallela* antennal transcriptome. Bioinformatics analysis supported the classification of these genes as members of the UGT superfamily, and sequence alignments enabled the prediction of structural features of the *H. parallela* antennal UGT proteins. Phylogenetic mapping revealed that *H. parallela* antennal UGTs are divided into eight groups. Specifically, *HparUGT9114* clusters in a conserved group with *SliUGT46A6* (Bozzolan *et al*., 2014), suggesting these UGTs might have similar functions in olfactory organs. In addition, qPCR analysis revealed that *HparUGT8312*, *HparUGT1265-1*, and *HparUGT3119* are highly expressed in antennae, indicating that their gene products may participate in specific olfactory functions. The data presented in this study provide an overview of dark black chafer UGTs, which will contribute to future functional studies of these enzymes.

Supplementary material

The supplementary material for this article can be found at https://doi.org/10.1017/S0007485318000068

Acknowledgements

This research was supported by the National Key Research and Development Program of China (2017YFD0200600) and the Natural Science Foundation of Jilin Province, P.R. China (20150309006NY). JJZ received research funding from BBSRC UK-China Partnering Awards (BB/J020281/1) and China-UK Cooperation Programme in Global Priorities (BB/L001683/1).

References

Ahn, S.J., Badenes-Pérez, F.R., Reichelt, M., Svatoš, A., Schneider, B., Gershenzon, J. & Heckel, D.G. (2011) Metabolic detoxification of capsaicin by UDP-glycosyltransferase in three *Helicoverpa* species. *Archives of Insect Biochemistry and Physiology* **78**, 104–118.

Ahn, S.J., Vogel, H. & Heckel, D.G. (2012) Comparative analysis of the UDP-glycosyltransferase multigene family in insects. *Insect Biochemistry and Molecular Biology* **42**, 133–147.

Altschul, S.F., Madden, T.L., Schäffer, A.A., Zhang, J., Zhang, Z., Miller, W. & Lipman, D.J. (1997) Gapped BLAST and PSI-BLAST: a new generation of protein database search programs. *Nucleic Acids Research* **25**, 3389–3402.

Barvkar, V.T., Pardeshi, V.C., Kale, S.M., Kadoo, N.Y. & Gupta, V.S. (2012) Phylogenomic analysis of UDP glycosyltransferase 1 multigene family in Linum usitatissimum identified genes with varied expression patterns. *BMC Genomics* **13**, 1471–2164.

Benton, R., Vannice, K.S. & Vosshall, L.B. (2007) An essential role for a CD36-related receptor in pheromone detection in Drosophila. *Nature* **450**, 289–293.

Biasini, M., Bienert, S., Waterhouse, A., Arnold, K., Studer, G., Schmidt, T., Kiefer, F., Cassarino, T.G., Bertoni, M., Bordoli, L. & Schwede, T. (2014). SWISS-MODEL: modelling protein tertiary and quaternary structure using evolutionary information. *Nucleic Acids Research* **42**, W252–W258.

Bock, K.W. (2016) The UDP-glycosyltransferase (UGT) superfamily expressed in humans, insects and plants: animal-plant arms-race and co-evolution. *Biochemical Pharmacology* **99**, 11–17.

Bozzolan, F., Siaussat, D., Maria, A., Durand, N., Pottier, M.A., Chertemps, T. & Maïbèche-Coisne, M. (2014) Antennal uridine diphosphate (UDP)-glycosyltransferases in a pest insect: diversity and putative function in odorant and xenobiotics clearance. *Insect Molecular Biology* **23**, 539–549.

Cartwright, A.M., Lim, E.K., Kleanthous, C. & Bowles, D.J. (2008) A kinetic analysis of regiospecific glucosylation by two glycosyltransferases of *Arabidopsis thaliana*: domain swapping to introduce new activities. *Journal of Biological Chemistry* **283**, 15724–15731.

Duan, M., Xiong, J., Lu, D., Wang, G. & Ai, H. (2016) Transcriptome sequencing analysis and functional identification of sex differentiation genes from the mosquito parasitic nematode, *Romanomermis wuchangensis*. *PLoS ONE* **11**, e0163127.

Durand, N., Carot-Sans, G., Chertemps, T., Montagné, N., Jacquin-Joly, E., Debernard, S. & Maïbèche-Coisne, M. (2010) A diversity of putative carboxylesterases are expressed in the antennae of the noctuid moth *Spodoptera littoralis*. *Insect Molecular Biology* **19**, 87–97.

Gasteiger, E., Gattiker, A., Hoogland, C., Ivanyi, I., Appel, R.D. & Bairoch, A. (2003) ExPASy: the proteomics server for in-depth protein knowledge and analysis. *Nucleic Acids Research* **31**, 3784–3788.

Hanser, H.I., Faure, P., Robert-Hazotte, A., Artur, Y., Duchamp-Viret, P., Coureaud, G. & Heydel, J.M. (2017) Odorant-odorant metabolic interaction, a novel actor in olfactory perception and behavioral responsiveness. *Scientific Reports* **7**, 10219.

He, P., Li, Z.Q., Liu, C.C., Liu, S.J. & Dong, S.L. (2014) Two esterases from the genus *Spodoptera* degrade sex pheromones and plant volatiles. *Genome* **57**, 201–208.

Heydel, J., Leclerc, S., Bernard, P., Pelczar, H., Gradinaru, D., Magdalou, J., Minn, A., Artur, Y. & Goudonnet, H. (2001) Rat olfactory bulb and epithelium UDP-glucuronosyltransferase 2A1 (UGT2A1) expression: *in situ* mRNA localization and quantitative analysis. *Molecular Brain Research* **90**, 83–92.

Heydel, J.M., Holsztynska, E.J., Legendre, A., Thiebaud, N., Artur, Y. & Le Bon, A.M. (2010) UDP-glucuronosyltransferases (UGTs) in neuro-olfactory tissues: expression, regulation, and function. *Drug Metabolism Reviews* **42**, 74–97.

Heydel, J.M., Coelho, A., Thiebaud, N., Legendre, A., Le Bon, A. M., Faure, P., Neiers, F., Artur, Y., Golebiowski, J. & Briand, L. (2013) Odorant-binding proteins and xenobiotic metabolizing enzymes: implications in olfactory perireceptor events. *The Anatomical Record-Advances in Integrative Anatomy and Evolutionary Biology* **296**, 1333–1345.

Huang, F.F., Chai, C.L., Zhang, Z., Liu, Z.H., Dai, F.Y., Lu, C. & Xiang, Z.H. (2008) The UDP-glucosyltransferase multigene family in *Bombyx mori*. *BMC Genomics* **27**, 1471–2164.

Ju, Q., Qu, M.J., Wang, Y., Jiang, X.J., Li, X., Dong, S.L. & Han, Z. J. (2012) Molecular and biochemical characterization of two odorant-binding proteins from dark black chafer, *Holotrichia parallela*. *Genome* **55**, 537–546.

Ju, Q., Li, X., Jiang, X.J., Qu, M.J., Guo, X.Q., Han, Z.J. & Li, F. (2014) Transcriptome and tissue-specific expression analysis of Obp and Csp genes in the dark black chafer. *Archives of Insect Biochemistry and Physiology* **87**, 177–200.

Kojima, W., Fujii, T., Suwa, M., Miyazawa, M. & Ishikawa, Y. (2010) Physiological adaptation of the Asian corn borer *Ostrinia furnacalis* to chemical defenses of its host plant, maize. *Journal of Insect Physiology* **56**, 1349–1355.

Krempl, C., Sporer, T., Reichelt, M., Ahn, S.J., Heidel-Fischer, H., Vogel, H., Heckel, D.G. & Joußen, N. (2016) Potential

detoxification of gossypol by UDP-glycosyltransferases in the two heliothine moth species *Helicoverpa armigera* and *Heliothis virescens*. *Insect Biochemistry and Molecular Biology* **71**, 49–57.

Lazard, D., Zupko, K., Poria, Y., Nef, P., Lazarovits, J., Horn, S., Khen, M. & Lancet, D. (1991) Odorant signal termination by olfactory UDP glucuronosyl transferase. *Nature* **349**, 790–793.

Leclerc, S., Heydel, J.M., Amossé, V., Gradinaru, D., Cattarelli, M., Artur, Y., Goudonnet, H., Magdalou, J., Netter, P., Pelczar, H. & Minn, A. (2002) Glucuronidation of odorant molecules in the rat olfactory system: activity, expression and age-linked modifications of UDP-glucuronosyltransferase isoforms, UGT1A6 and UGT2A1, and relation to mitral cell activity. *Molecular Brain Research* **107**, 201–213.

Lim, E.K., Baldauf, S., Li, Y., Elias, L., Worrall, D., Spencer, S.P., Jackson, R.G., Taguchi, G., Ross, J. & Bowles, D.J. (2003) Evolution of substrate recognition across a multigene family of glycosyltransferases in Arabidopsis. *Glycobiology* **13**, 139–145.

Luque, T., Okano, K. & O'Reilly, D.R. (2002) Characterization of a novel silkworm (*Bombyx mori*) phenol UDP-glucosyltransferase. *European Journal of Biochemistry* **269**, 819–825.

Mackenzie, P.I., Owens, I.S., Burchell, B., Bock, K.W., Bairoch, A., Bélanger, A., Fournel-Gigleux, S., Green, M., Hum, D. W. & Iyanagi, T. (1997) The UDP glycosyltransferase gene superfamily: recommended nomenclature update based on evolutionary divergence. *Pharmacogenetics* **7**, 255–269.

Mackenzie, P.I., Bock, K.W., Burchell, B., Guillemette, C., Ikushiro, S., Iyanagi, T., Miners, J.O., Owens, I.S. & Nebert, D.W. (2005) Nomenclature update for the mammalian UDP glycosyltransferase (UGT) gene superfamily. *Pharmacogenetics and Genomics* **15**, 677–685.

Magdalou, J., Fournel-Gigleux, S. & Ouzzine, M. (2010) Insights on membrane topology and structure/function of UDP-glucuronosyltransferases. *Drug Metabolism Reviews* **42**, 159–166.

Mayer, U., Ungerer, N., Klimmeck, D., Warnken, U., Schnölzer, M., Frings, S. & Möhrlen, F. (2008) Proteomic analysis of a membrane preparation from rat olfactory sensory cilia. *Chemical Senses* **33**, 145–162.

Miley, M.J., Zielinska, A.K., Keenan, J.E., Bratton, S.M., Radominska-Pandya, A. & Redinbo, M.R. (2007) Crystal structure of the cofactor-binding domain of the human phase II drug-metabolism enzyme UDP-glucuronosyltransferase 2B7. *Journal of Molecular Biology* **369**, 498–511.

Olender, T., Keydar, I., Pinto, J.M., Tatarskyy, P., Alkelai, A., Chien, M.S., Fishilevich, S., Restrepo, D., Matsunami, H., Gilad, Y. & Lancet, D. (2016) The human olfactory transcriptome. *BMC Genomics* **17**, 619.

Osmani, S.A., Bak, S. & Møller, B.L. (2009) Substrate specificity of plant UDP-dependent glycosyltransferases predicted from crystal structures and homology modelling. *Phytochemistry* **70**, 325–347.

Petersen, T.N., Brunak, S., von Heijne, G. & Nielsen, H. (2011) Signalp 4.0: discriminating signal peptides from transmembrane regions. *Nature Methods* **8**, 785–786.

Pfaffl, M.W. (2001) A new mathematical model for relative quantification in real-time RT-PCR. *Nucleic Acids Research* **29**, e45.

Radominska-Pandya, A., Bratton, S.M., Redinbo, M.R. & Miley, M.J. (2010) The crystal structure of human UDP-glucuronosyltransferase 2B7 C-terminal end is the first mammalian UGT target to be revealed: the significance for human UGTs from both the 1A and 2B families. *Drug Metabolism Reviews* **42**, 133–144.

Robertson, H.M., Martos, R., Sears, C.R., Todres, E.Z., Walden, K. K. & Nardi, J.B. (1999) Diversity of odourant binding proteins revealed by an expressed sequence tag project on male *Manduca sexta* moth antennae. *Insect Molecular Biology* **8**, 501–518.

Rützler, M. & Zwiebel, L.J. (2005) Molecular biology of insect olfaction: recent progress and conceptual models. *Journal of Comparative Physiology. A, Neuroethology, Sensory, Neural, and Behavioral Physiology* **191**, 777–790.

Sasai, H., Ishida, M., Murakami, K., Tadokoro, N., Ishihara, A., Nishida, R. & Mori, N. (2009) Species-specific glucosylation of DIMBOA in larvae of the rice Armyworm. *Bioscience, Biotechnology, and Biochemistry* **73**, 1333–1338.

Tamura, K., Stecher, G., Peterson, D., Filipski, A. & Kumar, S. (2013) MEGA6: molecular evolutionary genetics analysis version 6.0. *Molecular Biology and Evolution* **30**, 2725–2729.

Vogt, R.G. & Riddiford, L.M. (1981) Pheromone binding and inactivation by moth antennae. *Nature* **293**, 161–163.

Wang, Q., Hasan, G. & Pikielny, C.W. (1999) Preferential expression of biotransformation enzymes in the olfactory organs of Drosophila melanogaster, the antennae. *Journal of Biological Chemistry* **274**, 10309–10315.

Wang, S., Yi, J.K., Yang, S., Liu, Y., Zhang, J.H. & Xi, J.H. (2017) Identification and characterization of microRNAs expressed in antennae of *Holotrichia parallela* motschulsky and their possible roles in olfactory regulation. *Archives of Insect Biochemistry and Physiology* **94**, e21369.

Younus, F., Chertemps, T., Pearce, S.L., Pandey, G., Bozzolan, F., Coppin, C.W., Russell, R.J., Maïbèche-Coisne, M. & Oakeshott, J.G. (2014) Identification of candidate odorant degrading gene/enzyme systems in the antennal transcriptome of *Drosophila melanogaster*. *Insect Biochemistry and Molecular Biology* **53**, 30–43.

Zhang, J.H., Wang, S., Yang, S., Yi, J., Liu, Y. & Xi, J.H. (2016) Differential proteome analysis of the male and female antennae from *Holotrichia parallela*. *Archives of Insect Biochemistry and Physiology* **92**, 274–287.

Zhang, X., Zhang, Q.Y., Liu, D., Su, T., Weng, Y., Ling, G., Chen, Y., Gu, J., Schilling, B. & Ding, X. (2005) Expression of cytochrome p450 and other biotransformation genes in fetal and adult human nasal mucosa. *Drug Metabolism and Disposition* **33**, 1423–1428.

Zhou, J.J. (2010) Odorant-binding proteins in insects. *Vitamins and Hormones* **83**, 241–272.

Zhou, J.J., Field, L.M. & He, X.L. (2010). Insect odorant-binding proteins: do they offer an alternative pest control strategy? *Outlooks on Pest Management* **21**, 31–34.